
An Efficient Adversarial Attack for Tree Ensembles

Chong Zhang Huan Zhang Cho-Jui Hsieh

Department of Computer Science, UCLA

chongz@cs.ucla.edu, huan@huan-zhang.com, chohsieh@cs.ucla.edu

Abstract

We study the problem of efficient adversarial attacks on tree based ensembles such as gradient boosting decision trees (GBDTs) and random forests (RFs). Since these models are non-continuous step functions and gradient does not exist, most existing efficient adversarial attacks are not applicable. Although decision-based black-box attacks can be applied, they cannot utilize the special structure of trees. In our work, we transform the attack problem into a discrete search problem specially designed for tree ensembles, where the goal is to find a valid “leaf tuple” that leads to mis-classification while having the shortest distance to the original input. With this formulation, we show that a simple yet effective greedy algorithm can be applied to iteratively optimize the adversarial example by moving the leaf tuple to its neighborhood within hamming distance 1. Experimental results on several large GBDT and RF models with up to hundreds of trees demonstrate that our method can be thousands of times faster than the previous mixed-integer linear programming (MILP) based approach, while also providing smaller (better) adversarial examples than decision-based black-box attacks on general ℓ_p ($p = 1, 2, \infty$) norm perturbations. Our code is available at <https://github.com/chong-z/tree-ensemble-attack>.

1 Introduction

It has been widely studied that machine learning models are vulnerable to adversarial examples (Szegedy et al., 2013; Goodfellow et al., 2015; Athalye et al., 2018), where a small imperceptible perturbation on the input can easily alter the prediction of a model. A series of adversarial attack methods have been proposed on continuous models such as neural networks, which can be generally split into two types. The gradient based methods formulate the attack into an optimization problem on a specially designed loss function for attacks, where the gradient can be acquired through either back-propagation in the white-box setting (Carlini, Wagner, 2017; Madry et al., 2018), or numerical estimation in the soft-label black-box setting (Chen et al., 2017; Tu et al., 2018; Ilyas et al., 2018). The decision based (or hard-label black-box) methods only have access to the output label, which usually starts with an initial adversarial example and minimizes the perturbation along the decision boundary (Brendel et al., 2018; Brunner et al., 2018; Cheng et al., 2019, 2020; Chen et al., 2019c).

In this paper we study the problem of efficient adversarial attack on tree based ensembles such as gradient boosting decision trees (GBDT) and random forests (RFs), which have been widely used in practice (Chen, Guestrin, 2016; Ke et al., 2017; Zhang et al., 2017; Prokhorenkova et al., 2018). We minimize the perturbation to find the *smallest possible* attack, to uncover the true weakness of a model. Different from neural networks, tree based ensembles are non-continuous step functions and existing gradient based methods are not applicable. Decision based methods can be applied but they usually require a large number of queries and may easily fall into local optimum due to rugged decision boundary. In general, finding the exact minimal adversarial perturbation for tree ensembles is NP-complete (Kantchelian et al., 2015), and a feasible approximation solution is necessary to evaluate the robustness of large ensembles.

The major difficulty of attacking tree ensembles is that the prediction remains unchanged within regions on the input space, where the region could be large and makes continuous updates inefficient. To overcome this difficulty, we transform the continuous \mathbb{R}^d input space into a discrete $\{1, 2, \dots, N\}^K$ “leaf tuple” space, where N is the number of leaves per tree and K is the number of trees. On the leaf tuple space we define the distance between two input examples to be the number of trees that have different prediction leaves (i.e., hamming distance), and define the neighborhood of a tuple to be all valid tuples within a small hamming distance. In practice, we propose the attack that iteratively optimizes the adversarial leaf tuple by moving it to the best adversarial tuple within the neighborhood of distance 1. Intuitively we could reach a far away adversarial tuple through a series of smaller updates, based on the fact that each tree makes prediction independently.

In experiments, we compare $\ell_{1,2,\infty}$ norm perturbation metrics across 10 datasets, and show that our method is thousands of times faster than MILP (Kantchelian et al., 2015) on most of the large ensembles, and 3~72x faster than decision based and empirical attacks on all datasets while achieving a smaller distortion. For instance, with the standard (natural) GBDT on the MNIST dataset with 10 classes and 200 trees per class, our method finds the adversarial example with only 2.07 times larger ℓ_∞ perturbation than the optimal solution produced by MILP and only uses 0.237 seconds per test example, whereas MILP requires 375 seconds. As for other approximate attacks, SignOPT (Cheng et al., 2020) finds a 13.93 times larger ℓ_∞ perturbation (compared to MILP) using 3.7 seconds, HSJA (Chen et al., 2019c) achieves a 8.36 times larger ℓ_∞ perturbation using 1.8 seconds, and Cube (Andriushchenko, Hein, 2019) achieves a 4 times larger ℓ_∞ perturbation using 4.42 seconds. Additionally, although ℓ_p distance is widely used in previous attacks and a small ℓ_p perturbation is usually invisible, our method is general and can also be adapted to other distance metrics.

2 Background and Related Work

Problem Setting While the main idea can be applied to multi-class classification models and targeted attacks, for simplicity we consider a binary classification model $f : \mathbb{R}^d \rightarrow \{-1, 1\}$ consisting of K decision trees. Each tree t is a weak learner $f_t : \mathbb{R}^d \rightarrow \mathbb{R}$ of N leaves, and the ensemble returns the sign $f(x) = \text{sign}(\sum_{t=1}^K f_t(x))$. Given a victim input example x_0 with $y_0 = f(x_0)$, we want to find the **minimal adversarial perturbation** r_p^* , determining the **adversarial robustness** under ℓ_p norm:

$$r_p^* = \min_{\delta} \|\delta\|_p \quad \text{s.t.} \quad f(x_0 + \delta) \neq y_0. \quad (1)$$

Exact Solutions In general computing the exact (optimal) solution for Eq. (1) requires exponential time: Kantchelian et al. (2015) showed that the problem is NP-complete for general ensembles and proposed a MILP based method; On the other hand, faster algorithms exist for models of special form: Zhang et al. (2020) restricted both the input and prediction of every tree t to binary values $f_t : \{-1, 1\}^d \rightarrow \{-1, 1\}$ and provided an integer linear program (ILP) based formulation about 4 times faster than Kantchelian et al. (2015); Andriushchenko, Hein (2019) showed that the exact robustness of boosted decision stumps (i.e., *depth* = 1) can be solved in polynomial time; Chen et al. (2019b) proposed a polynomial time algorithm to solve a single decision tree.

Approximate Solutions To get a feasible solution for general models a series of methods have been proposed to compute the *lower bound* (**robustness verification**) and the *upper bound* (**adversarial attacks**) of r_p^* . Chen et al. (2019b) formulated the robustness verification problem into a max-clique problem on a multi-partite graph and produced the *lower bound* on ℓ_∞ ; Wang et al. (2020) extended the verification method and produced a *lower bound* on general ℓ_p norms; Lee et al. (2019) verified the ℓ_0 robustness on the randomly smoothed ensembles which is not directly related to our work. On the other hand, decision based attacks (Brendel et al., 2018; Brunner et al., 2018; Cheng et al., 2019, 2020; Chen et al., 2019c) can be applied here to produce an *upper bound* since they don’t have architecture or smoothness assumptions on $f(\cdot)$, however they are usually ineffective due to the discrete nature of tree models; Andriushchenko, Hein (2019) proposed the Cube attack for tree ensembles that does stochastic updates along the ℓ_∞ boundary, which typically achieves better results than decision based attacks; Yang et al. (2019) focused on the theoretical analysis of search space decomposition, and proposed RBA-Appr to search over a subset of the N^K convex polyhedrons containing training examples; Zhang et al. (2020) restricted both the input and prediction of all trees to binary values and provided a heuristic attack on ℓ_0 by assigning empirical weights to each feature, in both the white-box setting and a special “black-box” setting via training substitute models. In contrast,

Table 1: Key differences to prior adversarial attacks that are applicable to general tree ensembles.

| | SignOPT | HSJA | Cube | RBA-Appr | Ours |
|---------------------------|---------------------------------|-------------|-------------------|------------------|-----------------------|
| Access Level | | black-box | black-box | white-box + data | white-box |
| Search Space | | input space | input space | training data | leaf tuple space |
| Step Size | small steps in continuous space | | ℓ_0 boundary | N/A | one leaf node |
| Model Queries / iteration | 200 | 100~632 | 100 | N/A | ~ 1 (see §3.4.1) |

our method works on ensemble of general trees $f_t : \mathbb{R}^d \rightarrow \mathbb{R}$, and utilizes the special properties of tree models to produce a tighter *upper bound* on general ℓ_p ($p = 1, 2, \infty$) norms efficiently. Table 1 highlights our key differences to prior adversarial attacks that are applicable to general tree ensembles.

Robust Training To overcome the vulnerability, Kantchelian et al. (2015) proposed adversarial boosting by appending adversarial examples to the training dataset; Chen et al. (2019a) optimized the worst case perturbation through a max-min saddle point problem and effectively increased the minimal adversarial perturbation; Andriushchenko, Hein (2019) upper bounded the robust test error by the sum of the max loss of each tree, and proposed a training scheme by minimizing this upper bound; Recently Chen et al. (2019d) approximated the saddle point objective with a greedy heuristic algorithm and further increased the robustness. We consider both the standard (natural) models and the robustly trained models (Chen et al., 2019a) to demonstrate our performance on different settings.

3 Proposed Algorithm

We propose an iterative approach where the algorithm starts with an initial adversarial example x' s.t. $f(x') \neq y_0$ and greedily moves closer to x_0 . At each iteration we choose a new adversarial example x'_{new} within a small *neighborhood* around x' that has the minimum ℓ_p distance to x_0 . Formally we define the update rule below, and the algorithm stops if x'_{new} does not give smaller perturbation than x' . The key problem is to define the neighborhood so that Eq. (2) can be efficiently solved, and we provide an efficient formulation in following sections. We defer all the proofs to Appendix C.

$$x'_{\text{new}} = \underset{x}{\operatorname{argmin}} \|x - x_0\|_p \quad \text{s.t.} \quad x \in \text{Neighbor}(x'), f(x) \neq y_0. \quad (2)$$

3.1 Transform Continuous Input Space into Discrete Leaf Tuples

In most of the existing attacks, Eq. (2) is solved by a continuous optimization algorithm where the $\text{Neighbor}(x')$ (the region where we find an improved solution) is a small ℓ_p ball around the current solution x' . The major difficulty of attacking tree ensemble is that the model prediction will remain unchanged within a region (which may not be small) containing x' , so traditional continuous distance measurements are not suitable here. And if we define the neighborhood as a large ℓ_p ball, due to the non-continuity of trees, $f(x)$ becomes intractable to enumerate. To handle these difficulties we introduce the concept of leaf tuple and rewrite Eq. (2) into a discrete form. Given an input example $x = [x_1, \dots, x_d]$ the traverse starts from the root node of each tree. Each internal node of index i has two children and a feature split threshold (j^i, η^i) , and x will be passed to the left child if $x_{j^i} \leq \eta^i$ and to the right child otherwise. The leaf node has a prediction label v^i , and will output v^i when x reaches here. We use $\mathcal{C}(x) = (i^{(1)}(x), \dots, i^{(K)}(x))$ to denote the index tuple of K prediction leaves from input x . In general we use the subscript \cdot_j to denote the j^{th} dimension, and the superscripts \cdot^i or $\cdot^{(t)}$ to denote the i^{th} node and t^{th} tree respectively.

Definition 1. (Bounding Box) $B^i = [l_1^i, r_1^i] \times \dots \times [l_d^i, r_d^i]$ denotes the bounding box of node i , which is the region that x will fall into this node following the feature split thresholds along the traverse path, and each l and r is either $\pm\infty$ or equals to one η^{i_k} along the traverse path. We use $B(\mathcal{C}(x)) = \bigcap_{i \in \mathcal{C}(x)} B^i = \bigcap_{i \in \mathcal{C}(x)} [l_1^i, r_1^i] \times \dots \times \bigcap_{i \in \mathcal{C}(x)} [l_d^i, r_d^i]$ to denote the Cartesian product of the intersection of K bounding boxes on the ensemble.

Definition 2. (Valid Tuple) $\mathbb{C} = \{\mathcal{C}(x) \mid \forall x \in \mathbb{R}^d\}$ denotes the set of all possible tuples that correspond to at least one point in the input space, and $\mathcal{C} = (i^{(1)}, \dots, i^{(K)})$ is a *valid tuple* iff. $\mathcal{C} \in \mathbb{C}$.

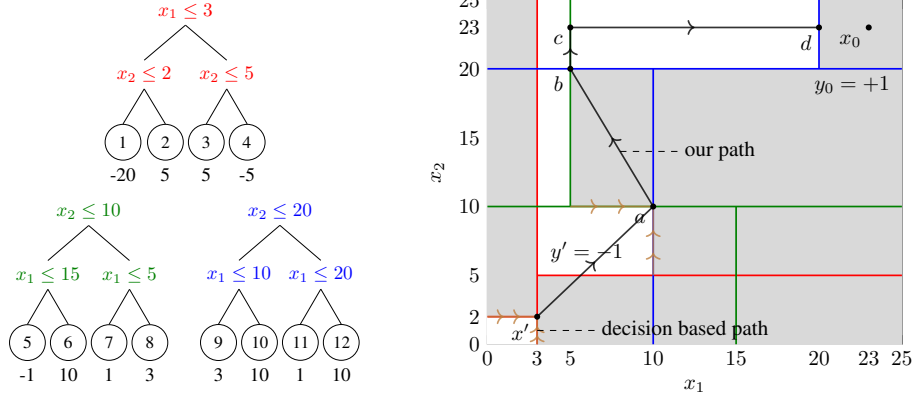


Figure 1: An ensemble defined on $[0, 25]^2$ and its corresponding decision boundaries on the input space. Numbers inside circles are indexes of leaves, and the number below each leaf is the corresponding prediction label v^i . For clarity we mark boundaries belong to tree 1, 2, 3 with red, green, and blue respectively, and fill $+1$ area with gray. x_0 is the victim example and x' is an initial adversarial example. Assume we are optimizing ℓ_1 perturbation, our method can reach d by changing one leaf of the tuple at a time (black arrows). On the other hand, decision based attacks update the solution along the decision boundary, and easily fall into local minimums such as x' and a (brown arrows) since they look only at the continuous neighborhood. To move from a to b , the path on decision boundary is $a \rightarrow (5, 10) \rightarrow b$, but since $a \rightarrow (5, 10)$ increases the distortion they won't find this path.

Theorem 1. (Chen et al., 2019b) The intersection $B(\mathcal{C})$ can also be written as the Cartesian product of d intervals (similar to B^i), and $\mathcal{C} \in \mathbb{C} \iff B(\mathcal{C}) \neq \emptyset \iff \forall i, j \in \mathcal{C}, B^i \cap B^j \neq \emptyset$. (These concepts were used in Chen et al. 2019b for verification instead of attack.)

Corollary 1. (Tuple to Example Distance) The shortest distance between a valid leaf tuple and an example, defined as $\text{dist}_p(\mathcal{C}, x_0) = \min_{x \in B(\mathcal{C})} \|x - x_0\|_p$, can be solved in $O(d)$ time.

Observe $\mathcal{C}(x) = \mathcal{C}(x')$, $\forall x \in B(\mathcal{C}(x'))$ and we can transform the intractable number of x into tractable number of leaf tuples \mathcal{C} . We abuse the notation $f(\mathcal{C})$ to denote the model prediction $\text{sign}(\sum_{i \in \mathcal{C}} v^i)$, which is a constant within $B(\mathcal{C})$. Combined with Corollary 1 we can rewrite Eq. (2) into the discrete form below. Neighbor(\mathcal{C}') denotes the *neighborhood* space around \mathcal{C}' , which is a set of leaf tuples that *close* to \mathcal{C}' in certain distance measurements. Fig. 1 presents an example to demonstrate that it's less likely to fall into local optimum on our newly defined neighborhood space.

$$\mathcal{C}'_{\text{new}} = \underset{\mathcal{C}}{\text{argmin}} \text{dist}_p(\mathcal{C}, x_0) \quad \text{s.t.} \quad \mathcal{C} \in \text{Neighbor}(\mathcal{C}') \cap \mathbb{C}, f(\mathcal{C}) \neq y_0. \quad (3)$$

3.2 Limitations of Naive Neighborhood Space Definitions

Now we discuss how to define Neighbor(\mathcal{C}') to facilitate our attack. Intuitively the space should be efficient to compute, and has a reasonable coverage to avoid falling into local minimums too easily. In this section we discuss two naive approaches that fail on these two properties, and provide empirical results in Table 2.

Enumerating all leaves is not efficient (NaiveLeaf): Given current adversarial example x' and its corresponding leaf tuple $\mathcal{C}' = (i^{(1)}, \dots, i^{(K)})$, an intuitive approach is to change a single $i^{(t)}$ to a different leaf $i_{\text{new}}^{(t)}$. However the resulting tuple may not be valid, and we will have to query the ensemble to get a valid tuple in \mathbb{C} . We provide a possible implementation in Appendix D.2 where we move x' to the closest point within $B_{\text{new}}^{i^{(t)}}$. NaiveLeaf requires multiple full model queries and takes $O(K \cdot 2^l \cdot Kl)$ time per iteration for K trees of depth l , which is too time consuming (see Table 2).

Mutating one feature at a time has poor coverage (NaiveFeature): Given current adversarial example x' and its corresponding leaf tuple \mathcal{C}' , another intuitive approach is to move x' outside of $B(\mathcal{C}')$ on each feature dimension. This approach is efficient since there are at most $2d$ neighborhood, and each neighborhood is only different by one tree (assuming unique split thresholds). However the

Table 2: Average ℓ_2 perturbation over 500 test examples on the standard (natural) GBDT models. ("*"): For a fair comparison we disabled the random noise optimization discussed in §3.5. Our LT-Attack searches in a subspace of NaiveLeaf so \bar{r}_{our} is slightly larger, but it is significantly faster.

| Standard GBDT ℓ_2 Perturbation | NaiveLeaf | | NaiveFeature | | LT-Attack (Ours)* | | Ours vs. NaiveLeaf | |
|--|-------------------------|-------|--------------|-------|------------------------|-------|--|---------|
| | \bar{r}_{leaf} | time | \bar{r} | time | \bar{r}_{our} | time | $\bar{r}_{\text{our}}/\bar{r}_{\text{leaf}}$ | Speedup |
| MNIST | .081 | 2.37s | .229 | .069s | .108 | .105s | 1.33 | 22.6X |
| F-MNIST | .080 | 3.93s | .181 | .061s | .096 | .224s | 1.20 | 17.5X |
| HIGGS | .008 | 3.17s | .011 | .023s | .009 | .031s | 1.13 | 102.3X |

method easily falls into local minimums due to the fact that each leaf is bounded by up to l features jointly, thus it's unlikely to reach certain leaves by only changing one feature at a time. Taking Fig. 1 as an example and assume we are at x' , notice that $B(\mathcal{C}(x')) = [0, 3] \times [0, 2]$ and the algorithm stops here since both neighborhood $\{(3 + \epsilon, 2), (3, 2 + \epsilon)\}$ are not adversarial examples.

3.3 Define Neighborhood Space by Hamming Distance

In this section we introduce a neighborhood space through discrete hamming distance, and show that it's fast to compute and has good coverage. We define the distance $D(\mathcal{C}, \mathcal{C}')$ between two tuples as the number of different leaves, and the neighborhood of \mathcal{C}' with distance h by

$$\text{Neighbor}_h(\mathcal{C}') = \{\mathcal{C} \mid \forall \mathcal{C} \in \mathbb{C}, D(\mathcal{C}, \mathcal{C}') = h\}. \quad (4)$$

The intuition is that each tree can be queried independently, and we want to utilize such property by limiting the number of affected search trees at each iteration. $\text{Neighbor}_h(\cdot)$ has a nice property where we can increase h for larger search scope, or decrease h to improve speed. Observe that $\text{Neighbor}_1(\mathcal{C}')$ is a subset of NaiveLeaf (minus invalid leaf tuples that requires an expensive model query), and a superset of NaiveFeature (plus leaf tuples that may affect multiple features). In experiments we are able to achieve good results with $\text{Neighbor}_1(\cdot)$, and we provide an empirical greedy algorithm in Appendix D.3 to estimate the minimal h required to reach the exact solution.

3.4 An Efficient Algorithm for Solving $\text{Neighbor}_1(\cdot)$

We propose Leaf Tuple attack (LT-Attack) in Algorithm 1 that efficiently solves Eq. (3) through two additional concepts $T_{\text{Bound}}(\cdot)$ and $\text{Neighbor}_1^{(t)}(\cdot)$ as defined below. Let \mathcal{C}' be any valid adversarial tuple, and assume unique feature split thresholds. By definition tuples in $\text{Neighbor}_1(\mathcal{C}')$ are only different from \mathcal{C}' by one leaf, and we use $\text{Neighbor}_1^{(t)}(\mathcal{C}')$ to denote the neighborhood that has different prediction leaf on tree t . Formally

$$\text{Neighbor}_1^{(t)}(\mathcal{C}') = \{\mathcal{C} \mid \mathcal{C}^{(t)} \neq \mathcal{C}'^{(t)}, \mathcal{C} \in \text{Neighbor}_1(\mathcal{C}')\}. \quad (5)$$

Definition 3. (*Bound Trees*) Let $x' \in B(\mathcal{C}')$ be the example that minimizes $\text{dist}_p(\mathcal{C}', x_0)$, we denote the indexes of trees that *bounds* x' by $T_{\text{Bound}}(\mathcal{C}') = \{t \mid \text{OnEdge}(x', B^{\mathcal{C}'^{(t)}}), \forall t \in \{1, \dots, K\}\}$. Here $\text{OnEdge}(x, B)$ is true iff. x equals to the left or the right bound of B on at least one dimension.

Definition 4. (*Advanced Neighborhood*) We denote the set of neighborhood with smaller (advanced) perturbation than \mathcal{C}' by $\text{Neighbor}_1^+(\mathcal{C}') = \{\mathcal{C} \mid \mathcal{C} \in \text{Neighbor}_1(\mathcal{C}'), \text{dist}_p(\mathcal{C}, x_0) < \text{dist}_p(\mathcal{C}', x_0)\}$.

Theorem 2. (*Bound Neighborhood*) Let $\text{Neighbor}_{\text{Bound}}(\mathcal{C}') = \bigcup_{t \in T_{\text{Bound}}(\mathcal{C}')} \text{Neighbor}_1^{(t)}(\mathcal{C}')$, then $\text{Neighbor}_1^+(\mathcal{C}') \subseteq \text{Neighbor}_{\text{Bound}}(\mathcal{C}')$.

Theorem 2 suggests that we can solve Eq. (3) by searching over $\text{Neighbor}_{\text{Bound}}(\mathcal{C}')$ since it is a superset of the advanced neighborhood which leads to smaller perturbation. In general the algorithm consists of an outer loop and an inner $\text{Neighbor}_{\text{Bound}}(\cdot)$ function. The outer loop iterates until no better adversarial example can be found, while the inner function generates bound neighborhood with distance 1. The inner function computes T_{Bound} and runs the top-down traverse for each $t \in T_{\text{Bound}}$ with the intersection of other $K - 1$ bounding boxes, denoted by $B^{(-t)}$. According to Theorem 1, a leaf node of t is guaranteed to form a valid tuple if it has non-empty intersection with $B^{(-t)}$.

To efficiently obtain $B^{(-t)}$ we cache K bounding boxes in B' , and for each feature dimension we maintain the sorted list of left and right bounds from K boxes respectively. Note that B^i of leaf node i

Algorithm 1: Our proposed LT-Attack for constructing adversarial examples.

Data: White-box model f , victim example x_0, y_0 , initial adversarial example x' .

```

1 begin
2    $r', C' \leftarrow \text{dist}_p(\mathcal{C}(x'), x_0), \mathcal{C}(x')$ ;
3    $B' \leftarrow \text{BuildSortedBoxes}(C', f)$ ;
4    $\triangleright O(Kl \log K)$  -  $B'$  maintains  $K$  sorted bounding
5     boxes on  $d$  feature dimensions.
6    $\text{has\_better\_neighbor} \leftarrow \text{True}$ ;
7   while  $\text{has\_better\_neighbor}$  do
8      $N_1 \leftarrow \text{Neighbor}_{\text{Bound}}(C', B', f)$ ;
9      $\triangleright$  See complexity in §3.4.1
10     $N'_1 \leftarrow \{C \mid C \in N_1, f(C) \neq y_0\}$ ;
11     $\triangleright O(|N_1|)$  -  $f(C)$  can be calculated from
12     $f(C')$  in  $O(1)$  using the diff leaf.
13     $r^*, C^* \leftarrow \underset{r, C}{\text{argmin}} \{\text{dist}_p(C, x_0) \mid C \in N'_1\}$ ;
14     $\triangleright O(l|N'_1|)$  -  $\text{dist}_p(C, x_0)$  can be calculated
15    from  $r'$  in  $O(l)$  using the diff leaf.
16     $\text{has\_better\_neighbor} \leftarrow r^* < r'$ ;
17    if  $\text{has\_better\_neighbor}$  then
18       $r', C' \leftarrow r^*, C^*$ ;
19       $B' \leftarrow B'.\text{ReplaceBox}(C^*)$ ;
20       $\triangleright O(l \log K)$  - Remove and add one box.
21    end
22  end
23  return  $r', C'$ 
24 end

```

```

17 Function  $\text{Neighbor}_{\text{Bound}}(C', B', f)$ :
18    $N_1 \leftarrow \emptyset$ ;
19    $T \leftarrow T_{\text{Bound}}(C', B')$ ;
20    $\triangleright O(d \log K)$  - Need  $O(\log K)$  to get the first
21     (tightest) tree on each dimension, and assume
22      $C'$  caches the closet  $x'$  to  $x_0$ . We give a
23     closer complexity analysis for  $|T_{\text{Bound}}(\cdot)|$  in
24     the following section.
25   for  $t \in T$  do
26      $B^{(-t)} \leftarrow B'.\text{RemoveBox}(t)$ ;
27      $\triangleright O(l \log K)$  - Remove the bounding box of
28     tree  $t$  from the sorted list (lazily), the
29     box has at most  $l$  non-infinite dimensions.
30      $I \leftarrow \{i \mid B^i \cap B^{(-t)} \neq \emptyset, i \in S^{(t)} \setminus C'^{(t)}\}$ ;
31      $\triangleright O(2^l)$  - Traverse tree  $t$  top-down and
32     return leaves for  $\text{Neighbor}_1^{(t)}(C')$ .  $S^{(t)}$ 
33     denotes the set of leaves of tree  $t$ .
34      $N_1 \leftarrow N_1 \cup \{C' \mid C'^{(t)} \leftarrow i, i \in I\}$ ;
35      $\triangleright O(|I|)$  - Construct the neighborhood tuple
36     by replacing the  $t_{\text{th}}$  leaf. In practice,
37     we only need to return the diff  $(t, i)$ .
38   end
39   return  $N_1$ 
40 end

```

comes from feature split thresholds along the top-down traverse path, thus it has at most l non-infinite dimensions, where l is the depth of the tree. In conclusion we can add/remove a bounding box B^i to/from B' in $O(l \log K)$ time. We provide time complexity for most operations in Algorithm 1 inline, and give a detailed analysis for the size of $\text{Neighbor}_{\text{Bound}}(C')$ in the next section. See Appendix D.1 for the algorithm generating random initial adversarial examples.

3.4.1 Size of the Bound Neighborhood

Our LT-Attack enumerates all leaf tuples in the bound neighborhood at each iteration, thus the complexity of each iteration largely depends on the size of $\text{Neighbor}_{\text{Bound}}(C')$. In this section we analyze the size $|\text{Neighbor}_{\text{Bound}}(C')|$ and show it will not be too large on real datasets.

Corollary 2. (*Size of $\text{Neighbor}_1^{(t)}(C')$*) Let $k^{(t)} = |\{\eta \in B_j^{(-t)}, (j, \eta) \in H(t)\}|$ be the number of feature split thresholds inside $B^{(-t)}$, we have $|\text{Neighbor}_1^{(t)}(C')| \leq 2^{\min(k^{(t)}, l)} - 1$. Here $B^{(-t)} = \bigcap_{i \in C', i \neq C'^{(t)}} B^i$ and $H(t)$ denotes the set of feature split thresholds on all internal nodes of tree t .

In practice, $k^{(t)} \ll l$ since $B^{(-t)}$ is the intersection of $K - 1$ bounding boxes and only covers a small region of the input space \mathbb{R}^d . $|T_{\text{Bound}}(C')| \leq d$ and is also usually small in real datasets, which can be explained by the intuition that some features are less *important* and could reach the same value as x_0 easily. Both $|T_{\text{Bound}}(C')|$ and $|\text{Neighbor}_1^{(t)}(C')|$ characterize the complexity of $|\text{Neighbor}_{\text{Bound}}(C')|$. We provide empirical statistics in Appendix A, which suggests that $|\text{Neighbor}_{\text{Bound}}(C')|$ has the similar complexity as a single full model query. For instance, on the MNIST dataset with 784 features and 400 trees we have mean $|\text{Neighbor}_{\text{Bound}}(C')| \approx 367.9$, and the algorithm stops in ~ 159.4 iterations when it cannot find a better neighborhood. As a comparison, decision based methods usually require hundreds of full model queries per iteration to estimate the update direction.

3.4.2 Convergence Guarantee with $\text{Neighbor}_1(\cdot)$

In this section \bar{C} denotes the converged tuple when the outer loop stops, and we discuss the property of the converged solution. Trivially \bar{C} has the minimal adversarial perturbation within $\text{Neighbor}_1(\bar{C})$, and we can show that the guarantee is actually stronger.

Table 3: Average ℓ_∞ and ℓ_2 perturbation of 500 test examples (or the entire test set when its size is less than 500) on **standard (natural) GBDT models**. Datasets are ordered by training data size. **Bold** and **blue** highlight the best and the second best entries respectively (not including MILP). ("*"): Average of 50 examples due to long running time. ("*"): HSJA has fluctuating running time.

| Standard GBDT | SignOPT | | HSJA | | RBA-Appr | | Cube | | LT-Attack (Ours) | | MILP | | Ours vs. MILP | |
|---------------|-----------|--------------|-------------|--------------|-------------|---------------|-------------|-------|------------------------|--------------|-------|--------|----------------------------|----------|
| | \bar{r} | time | \bar{r} | time | \bar{r} | time | \bar{r} | time | \bar{r}_{our} | time | r^* | time | \bar{r}_{our}/r^* | Speedup |
| breast-cancer | .258 | .308s | .256 | .070s | .247 | .0008s | .530 | .230s | .235 | .001s | .222 | .013s | 1.06 | 13X |
| diabetes | .083 | .343s | .078 | .066s | .113 | .0009s | .080 | .240s | .059 | .002s | .056 | .084s | 1.05 | 42X |
| MNIST2-6 | .480 | 2.73s | .277 | 1.23s | .963 | .155s | .143 | 2.43s | .097 | .222s | .065 | 28.7s | 1.49 | 129.3X |
| ijcnn | .043 | .313s | .043 | .096s | .074 | .020s | .035 | .334s | .033 | .007s | .031 | 6.60s | 1.06 | 942.9X |
| MNIST | .195 | 3.70s | .117 | 28.7s* | .983 | 4.11s | .056 | 4.42s | .029 | .237s | .014 | 375s* | 2.07 | 1582.3X |
| F-MNIST | .155 | 4.38s | .065 | 1.81s | .607 | 5.55s | .038 | 5.45s | .028 | .370s | .013 | 15min* | 2.15 | 2473X |
| webspam | .013 | 1.01s | .023 | .445s | .051 | .720s | .003 | .866s | .001 | .051s | .0008 | 27.5s | 1.25 | 539.2X |
| covtype | .047 | .508s | .074 | .209s | .086 | 3.05s | .036 | .958s | .032 | .038s | .028 | 10min* | 1.14 | 15736.8X |
| HIGGS | .009 | .465s | .012 | .157s | .099 | 55.3s* | .005 | .862s | .004 | .036s | .004 | 52min* | 1.00 | 87166.7X |

| Standard GBDT | SignOPT | | HSJA | | RBA-Appr | | Cube | | LT-Attack (Ours) | | MILP | | Ours vs. MILP | |
|---------------|-------------|-------|-----------|--------------|-----------|---------------|-------------|-------|------------------------|--------------|-------|--------|----------------------------|----------|
| | \bar{r} | time | \bar{r} | time | \bar{r} | time | \bar{r} | time | \bar{r}_{our} | time | r^* | time | \bar{r}_{our}/r^* | Speedup |
| breast-cancer | .310 | .811s | .370 | .072s | .352 | .0008s | .678 | .248s | .283 | .001s | .280 | .011s | 1.01 | 11X |
| diabetes | .106 | .650s | .123 | .064s | .158 | .001s | .136 | .269s | .077 | .003s | .073 | .055s | 1.05 | 18.3X |
| MNIST2-6 | 2.18 | 7.29s | 2.45 | 1.54s | 3.98 | .155s | .801 | 3.73s | .245 | .235s | .183 | 2.52s | 1.34 | 10.7X |
| ijcnn | .051 | .544s | .052 | .094s | .112 | .020s | .067 | .355s | .044 | .010s | .043 | 2.18s | 1.02 | 218X |
| MNIST | 1.20 | 8.71s | 1.45 | 23.7s* | 5.38 | 4.11s | .310 | 6.67s | .072 | .243s | .043 | 32.5s | 1.67 | 133.7X |
| F-MNIST | .870 | 9.57s | .581 | 2.03s | 3.85 | 5.48s | .225 | 9.20s | .073 | .400s | .049 | 49.3s | 1.49 | 123.3X |
| webspam | .023 | 3.26s | .112 | .529s | .128 | .721s | .009 | 1.04s | .002 | .053s | .002 | 3.17s | 1.00 | 59.8X |
| covtype | .061 | .976s | .123 | .217s | .129 | 3.03s | .070 | 1.06s | .045 | .039s | .042 | 237s | 1.07 | 6076.9X |
| HIGGS | .015 | 1.02s | .015 | .154s | .196 | 55.5s* | .013 | .905s | .008 | .037s | .007 | 13min* | 1.14 | 20621.6X |

Theorem 3. (Convergence Guarantee) Let $V^+ = \{i \mid i \in \mathcal{C}, \mathcal{C} \in \text{Neighbor}_1^+(\bar{\mathcal{C}})\}$ be the union of leaves appeared in the advanced neighborhood $\text{Neighbor}_1^+(\bar{\mathcal{C}})$ (Definition 4), then

$\bar{\mathcal{C}}$ is the optimum adversarial tuple within valid combinations of V^+ .

Note that V^+ is the union of leaves, and leaves from multiple tuples of distance 1 could form a new valid tuple of larger distance to $\bar{\mathcal{C}}$ (by combining the different leaves together). In other words Theorem 3 suggests that our solution is not only a local optimal in $\text{Neighbor}_1(\bar{\mathcal{C}})$, but also better than certain tuples in $\text{Neighbor}_h(\bar{\mathcal{C}})$ with $h > 1$. In our illustrated example Fig. 1, assume the algorithm converged at $\bar{\mathcal{C}} = \mathcal{C}(a) = (4, 5, 9)$ on ℓ_∞ norm, here $\text{Neighbor}_1^+(\mathcal{C}(a)) = \{(4, 8, 9), (4, 5, 10)\}$. Theorem 3 claims that there is no better adversarial tuple from any valid combinations within $V^+ = \{4, 5, 8, 9, 10\}$ such as $(4, 8, 10)$, even though it is from $\text{Neighbor}_2(\bar{\mathcal{C}})$.

3.5 Implementation Details

For the initial point, we draw 20 random initial adversarial examples from a Gaussian distribution, and optimize with a fine-grained binary search before feeding to the proposed algorithm. We return the best adversarial example found among them (see Appendix D.1 for details). The ensemble is likely to contain duplicate feature split thresholds even though it's defined on \mathbb{R}^d , for example it may come from the image space $[255]^d$ and scaled to \mathbb{R}^d . Duplicate split thresholds are problematic since we cannot move across the threshold without affecting multiple trees, and to overcome the issue we use a relaxed version of $\text{Neighbor}_1(\cdot)$ to allow changing multiple trees at one iteration, as long as it's caused by the same split threshold. When searching for the best neighborhood it's likely to have perturbation ties in ℓ_∞ and ℓ_1 norm, in this case we use a secondary ℓ_2 norm to break the tie. Eq. (3) looks for the best tuple across all neighborhood which may be unnecessary at early stage of iterations. To improve the efficiency we sort feature dimensions by $\text{abs}(x' - x_0)$ (large first), and terminate the search earlier if a better tuple was found in the top 1 feature. To escape converged local minimums we change each coordinate to a nearby value from Gaussian distribution with 0.1 probability, and continue the iteration if a better adversarial example was found within 300 trials.

4 Experimental Results

We evaluate the proposed algorithm on 9 public datasets (Smith et al., 1988; Lecun et al., 1998; Chang, Lin, 2011; Wang et al., 2012; Baldi et al., 2014; Xiao et al., 2017; Dua, Graff, 2017) with both the standard (natural) GBDT and RF models, and on an additional 10th dataset (Bosch, 2016) with

Table 4: Average ℓ_∞ and ℓ_2 perturbation of 5000 test examples (or the entire test set when its size is less than 5000) on **robustly trained GBDT models**. Datasets are ordered by training data size. **Bold** and **blue** highlight the best and the second best entries respectively (not including MILP). ("*" / "★"): Average of 1000 / 500 examples due to long running time.

| Robust GBDT | SignOPT | | HSJA | | RBA-Appr | | Cube | | LT-Attack (Ours) | | MILP | | Ours vs. MILP | |
|----------------------------|-------------|-------|-----------|--------------|-----------|--------------|-------------|-------|------------------------|--------------|-------|--------|----------------------------|----------|
| ℓ_∞ Perturbation | \bar{r} | time | \bar{r} | time | \bar{r} | time | \bar{r} | time | \bar{r}_{our} | time | r^* | time | \bar{r}_{our}/r^* | Speedup |
| breast-cancer | .403 | .371s | .405 | .073s | .405 | .002s | .888 | .238s | .404 | .002s | .401 | .010s* | 1.01 | 5.6X |
| diabetes | .119 | .364s | .123 | .068s | .138 | .001s | .230 | .239s | .113 | .003s | .112 | .039s* | 1.01 | 14.4X |
| MNIST2-6 | .588 | 3.06s | .470 | 1.30s | .671 | .137s | .337 | 2.15s | .333 | .275s | .313 | 177s* | 1.06 | 641.6X |
| ijcnn | .032 | .353s | .030 | .105s | .032 | .018s | .027 | .313s | .025 | .006s | .022 | 4.24s* | 1.14 | 759.6X |
| MNIST | .513 | 3.93s | .389 | 1.68s | .690 | 6.42s | .296 | 3.95s | .290 | .234s | .270 | 20min* | 1.07 | 5067.5X |
| F-MNIST | .254 | 4.31s | .154 | 1.79s | .596 | 7.83s | .101 | 4.45s | .095 | .412s | .076 | 74min* | 1.25 | 10778.5X |
| webspam | .047 | 1.00s | .043 | 4.14s | .061 | .641s | .020 | .756s | .017 | .031s | .015 | 129s* | 1.13 | 4129.4X |
| covtype | .064 | .540s | .080 | .186s | .093 | 3.61s | .055 | .720s | .047 | .047s | .045 | 14min* | 1.04 | 17164.9X |
| bosch | .343 | 3.28s | .337 | 1.42s | .533 | 1.22s | .158 | 2.49s | .143 | .213s | .100 | 237s* | 1.43 | 1112X |
| HIGGS | .015 | .466s | .016 | .134s | .048 | 72.4s* | .012 | .644s | .01 | .050s | .009 | 73min* | 1.11 | 87149.2X |

| Robust GBDT | SignOPT | | HSJA | | RBA-Appr | | Cube | | LT-Attack (Ours) | | MILP | | Ours vs. MILP | |
|-----------------------|-------------|-------|-------------|--------------|-------------|--------------|-------------|-------|------------------------|--------------|-------|--------|----------------------------|----------|
| ℓ_2 Perturbation | \bar{r} | time | \bar{r} | time | \bar{r} | time | \bar{r} | time | \bar{r}_{our} | time | r^* | time | \bar{r}_{our}/r^* | Speedup |
| breast-cancer | .437 | .711s | .449 | .069s | .436 | .002s | .940 | .239s | .434 | .002s | .431 | .011s* | 1.01 | 5.2X |
| diabetes | .142 | .591s | .150 | .061s | .161 | .003s | .274 | .240s | .133 | .005s | .132 | .025s* | 1.01 | 4.8X |
| MNIST2-6 | 2.97 | 7.37s | 3.32 | 1.28s | 2.95 | .156s | 1.31 | 3.19s | .971 | .438s | .762 | 25.0s* | 1.27 | 57.1X |
| ijcnn | .033 | .572s | .035 | .096s | .040 | .014s | .042 | .307s | .030 | .006s | .025 | 853s* | 1.20 | 140.3X |
| MNIST | 3.08 | 9.14s | 3.04 | 1.61s | 4.07 | 5.11s | 1.33 | 6.26s | .932 | .291s | .670 | 7min* | 1.39 | 1523.6X |
| F-MNIST | 1.67 | 9.27s | 1.34 | 1.64s | 3.72 | 7.01s | .500 | 7.01s | .310 | .385s | .233 | 231s* | 1.33 | 600.8X |
| webspam | .097 | 3.24s | .100 | .431s | .148 | .589s | .068 | .869s | .041 | .034s | .035 | 28.3s* | 1.17 | 840.6X |
| covtype | .076 | 1.11s | .104 | .196s | .137 | 3.26s | .096 | .726s | .062 | .047s | .058 | 9min* | 1.07 | 11183.1X |
| bosch | .750 | 9.62s | 2.33 | 1.54s | 1.45 | 1.21s | .480 | 3.84s | .258 | .232s | .214 | 28.0s* | 1.21 | 120.7X |
| HIGGS | .020 | .879s | .020 | .128s | .085 | 66.5s* | .023 | .580s | .016 | .045s | .014 | 24min* | 1.14 | 31715.5X |

the robustly trained GBDT. Datasets have a mix of small/large scale and binary/multi classification (statistics in Appendix A), and are normalized to $[0, 1]$ to make results comparable across datasets. We order datasets by training data size in all of our tables, where HIGGS is the largest dataset with 10.5 million training examples. All GBDTs were trained using the XGBoost framework (Chen, Guestrin, 2016) and we use the models provided by Chen et al. (2019b) as target models (except bosch). We compare with the following existing adversarial attacks that are applicable to tree ensembles:

- *SignOPT* (Cheng et al., 2020): The decision based attack that constructs adversarial examples based on hard-label black-box queries. We report the average distortion, denoted as \bar{r} in the results (since the norm of adversarial example is an upper bound of minimal adversarial perturbation r^*).
- *HSJA* (Chen et al., 2019c): Another decision based attack for constructing adversarial examples.
- *RBA-Appr* (Yang et al., 2019): An approximate attack for tree ensembles that constructs adversarial examples by searching over training examples of the opposite class.
- *Cube* (Andriushchenko, Hein, 2019): An empirical attack for tree ensembles that constructs adversarial examples by stochastically changing a few coordinates to the ℓ_∞ boundary, and accepts the change if it decreases the functional margin. The method provides good experimental results in general, but lacks theoretical guarantee and could be unreliable on certain datasets such as breast-cancer. Cube doesn't support ℓ_2 objective by default and we report the ℓ_2 perturbation of the constructed adversarial examples from ℓ_∞ objective attacks.
- *LT-Attack (Ours)*: Our proposed attack that constructs adversarial examples for tree ensembles. We report the average distortion of the adversarial examples, denoted as \bar{r}_{our} in the results.
- *MILP* (Kantchelian et al., 2015): The mixed-integer linear programming based method provides the exact minimal adversarial perturbation r^* but could be very slow on large models.

We run our experiments with 20 threads per task. Conventionally black-box attacks measure efficiency by the number of queries, here we compare running time since it's difficult to quantify queries for white-box attacks. To minimize the efficiency variance between programming languages we feed an XGBoost model (Chen, Guestrin, 2016) to SignOPT, HSJA, and Cube, which has an efficient C++ implementation and supports multi-threading batch query. MILP uses a thin wrapper around the Gurobi Solver (Gurobi Optimization, 2020). Baseline methods spend majority of time on XGBoost model inference rather than Python code. For instance, on Fashion-MNIST, SignOPT, HSJA, Cube spent 72.8%, 57.3%, 73.4% of runtime in XGBoost library (C++) calls, respectively. HSJA and

Table 5: Average ℓ_2 perturbation over 100 test examples on the **standard (natural) random forests (RF) models**. Datasets are ordered by training data size. **Bold** and **blue** highlight the best and the second best entries respectively (not including MILP).

| Standard RF ℓ_2 Perturbation | Cube | | LT-Attack (Ours) | | MILP | | Ours vs. MILP | |
|--------------------------------------|-----------|-------|------------------------|--------------|-------|-------|----------------------------|---------|
| | \bar{r} | time | \bar{r}_{our} | time | r^* | time | \bar{r}_{our}/r^* | Speedup |
| breast-cancer | 1.03 | .224s | .413 | .001s | .402 | .008s | 1.03 | 8X |
| diabetes | .260 | .285s | .151 | .003s | .146 | .042s | 1.03 | 14X |
| MNIST2-6 | .439 | 2.13s | .207 | .045s | .194 | .071s | 1.07 | 1.6X |
| ijcnn | .046 | .336s | .028 | .003s | .028 | .185s | 1.00 | 61.7X |
| MNIST | .057 | 2.88s | .018 | .057s | .018 | 4.56s | 1.00 | 80X |
| F-MNIST | .141 | 3.51s | .066 | .080s | .066 | 7.44s | 1.00 | 93X |
| webspam | .005 | .704s | .003 | .033s | .003 | .664s | 1.00 | 20.1X |
| covtype | .087 | .700s | .055 | .040s | .055 | 30.1s | 1.00 | 752.5X |
| HIGGS | .015 | .423s | .009 | .013s | .009 | 6.66s | 1.00 | 512.3X |

SignOPT start with 1 initial adversarial example and run 100~632 and 200 queries per iteration respectively to approximate the gradient, and Cube uses 20 initial examples which utilizes batch query. In Table 3 and Table 4 we show the empirical comparisons on ℓ_∞ and ℓ_2 , and provide ℓ_1 results as well as the attack success rate in Appendix B due to the space limit. We can see that our method provides a tight upper bound \bar{r}_{our} compared to the exact r^* from MILP, which means that the adversarial examples found are very close to the one with minimal adversarial perturbation, and our method achieved 1,000~80,000x speedup on some large models such as HIGGS. Our bound is tight especially in the ℓ_2 case. For instance, on Fashion-MNIST our \bar{r}/r^* ratio is 1.49x and 1.33x for standard and robustly trained models respectively, while the respective Cube ratio is 4.59x and 2.15x using ~21x time, and the respective HSJA ratio is 11.86x and 5.75x using ~4.5x time. For completeness we also include verification results (Chen et al., 2019b; Wang et al., 2020) in Appendix B since they are not directly comparable to adversarial attacks (they output lower bounds of the minimal adversarial perturbation while attacks aim to output an upper bound). To demonstrate the capability on general tree based ensembles we also conduct experiments on the standard (natural) random forests (RFs). We present the average ℓ_2 perturbation in Table 5, where the \bar{r}_{our}/r^* ratio is close to 1 across all datasets. Additional experimental results on ℓ_∞ perturbation can be found in Appendix B.1, and we include model parameters as well as statistics in Appendix A.

To study the impact of using different number of initial examples, we conduct the experiments with $\{1, 2, 4, 6, 10, 20, 40\}$ initial examples on SignOPT, HSJA, Cube, and LT-Attack, allocating 2 threads per task. We report the smallest (best) adversarial perturbation among those initial examples. Using more initial examples could lead to smaller (better) adversarial perturbation, but requires linearly increasing computational cost. Fig. 2 presents the ℓ_2 perturbation vs. runtime per test example in log scale, where our method is able to construct small (good) adversarial examples (y-axis) with a few initial examples, and can be orders of magnitude faster than other methods in the meantime (x-axis).

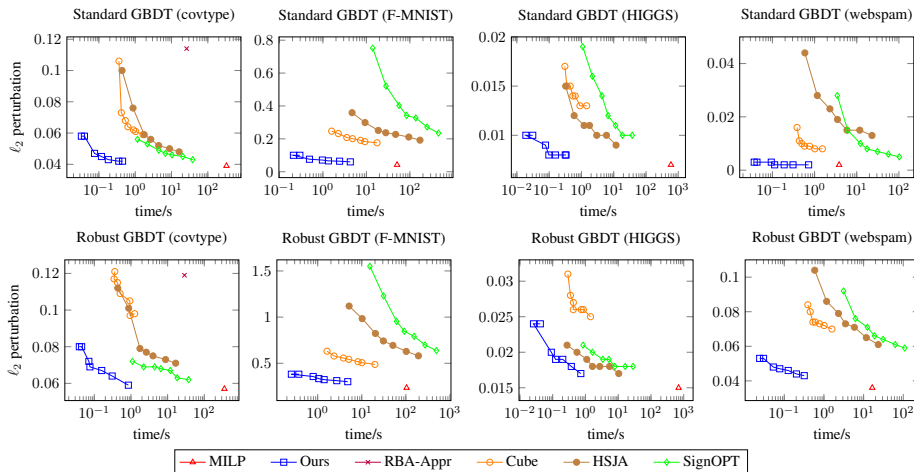


Figure 2: Average ℓ_2 perturbation of 50 test examples vs. runtime per test example in log scale. Methods on the bottom-left corner are better.

Broader Impact

To the best of our knowledge, this is the first practical attack algorithm (in terms of both computational time and solution quality) that can be used to evaluate the robustness of tree ensembles. The study of robustness training algorithms for tree ensemble models have been difficult due to the lack of attack tools to evaluate their robustness, and our method can serve as the benchmark tool for robustness evaluation (similar to FGSM, PGD and C&W attacks for neural networks) (Goodfellow et al., 2015; Madry et al., 2018; Carlini, Wagner, 2017) to stimulate the research in the robustness of tree ensembles.

Acknowledgments and Disclosure of Funding

We acknowledge the support by NSF IIS-1901527, IIS-2008173, ARL-0011469453, Google Cloud and Facebook.

References

- Andriushchenko Maksym, Hein Matthias.* Provably robust boosted decision stumps and trees against adversarial attacks // *Advances in Neural Information Processing Systems* 32. 2019. 13017–13028.
- Athalye Anish, Carlini Nicholas, Wagner David A.* Obfuscated Gradients Give a False Sense of Security: Circumventing Defenses to Adversarial Examples // *ICML*. 2018.
- Baldi Pierre, Sadowski Peter, Whiteson D. O.* Searching for exotic particles in high-energy physics with deep learning. // *Nature communications*. 2014. 5. 4308.
- Bosch .* Bosch Production Line Performance. 2016. <https://www.kaggle.com/c/bosch-production-line-performance/data>.
- Brendel Wieland, Rauber Jonas, Bethge Matthias.* Decision-Based Adversarial Attacks: Reliable Attacks Against Black-Box Machine Learning Models // *International Conference on Learning Representations*. 2018.
- Brunner Thomas, Diehl Frederik, Truong-Le Michael, Knoll Alois.* Guessing Smart: Biased Sampling for Efficient Black-Box Adversarial Attacks // *2019 IEEE/CVF International Conference on Computer Vision (ICCV)*. 2018. 4957–4965.
- Carlini Nicholas, Wagner David A.* Towards Evaluating the Robustness of Neural Networks // *2017 IEEE Symposium on Security and Privacy (SP)*. 2017. 39–57.
- Chang Chih-Chung, Lin Chih-Jen.* LIBSVM: A library for support vector machines // *ACM Transactions on Intelligent Systems and Technology*. 2011. 2. 27:1–27:27. Software available at <http://www.csie.ntu.edu.tw/~cjlin/libsvm>.
- Chen Hongge, Zhang Huan, Boning Duane S., Hsieh Cho-Jui.* Robust Decision Trees Against Adversarial Examples // *ICML*. 2019a. 1122–1131.
- Chen Hongge, Zhang Huan, Si Si, Li Yang, Boning Duane, Hsieh Cho-Jui.* Robustness Verification of Tree-based Models // *Advances in Neural Information Processing Systems* 32. 2019b. 12317–12328.
- Chen Jianbo, Jordan Michael I., Wainwright Martin J.* HopSkipJumpAttack: A Query-Efficient Decision-Based Adversarial Attack // *arXiv preprint arXiv:1904.02144*. 2019c.
- Chen Pin-Yu, Zhang Huan, Sharma Yash, Yi Jinfeng, Hsieh Cho-Jui.* ZOO: Zeroth Order Optimization Based Black-box Attacks to Deep Neural Networks without Training Substitute Models // *Proceedings of the 10th ACM Workshop on Artificial Intelligence and Security*. 2017.
- Chen Tianqi, Guestrin Carlos.* XGBoost: A Scalable Tree Boosting System // *Proceedings of the 22nd ACM SIGKDD International Conference on Knowledge Discovery and Data Mining*. New York, NY, USA: Association for Computing Machinery, 2016. 785–794. (KDD '16).

- Chen Yizheng, Wang Shiqi, Jiang Weifan, Cidon Asaf, Jana Suman.* Training Robust Tree Ensembles for Security. 2019d.
- Cheng Minhao, Le Thong, Chen Pin-Yu, Zhang Huan, Yi JinFeng, Hsieh Cho-Jui.* Query-Efficient Hard-label Black-box Attack: An Optimization-based Approach // International Conference on Learning Representations. 2019.
- Cheng Minhao, Singh Simranjit, Chen Patrick H., Chen Pin-Yu, Liu Sijia, Hsieh Cho-Jui.* Sign-OPT: A Query-Efficient Hard-label Adversarial Attack // International Conference on Learning Representations. 2020.
- Dua Dheeru, Graff Casey.* UCI Machine Learning Repository. 2017.
- Goodfellow Ian J., Shlens Jonathon, Szegedy Christian.* Explaining and Harnessing Adversarial Examples // CoRR. 2015. abs/1412.6572.
- Gurobi Optimization LLC.* Gurobi Optimizer Reference Manual. 2020.
- Ilyas Andrew, Engstrom Logan, Athalye Anish, Lin Jessy.* Black-box Adversarial Attacks with Limited Queries and Information // ICML. 2018.
- Kantchelian Alex, Tygar J. Doug, Joseph Anthony D.* Evasion and Hardening of Tree Ensemble Classifiers // ICML. 2015.
- Ke Guolin, Meng Qi, Finley Thomas, Wang Taifeng, Chen Wei, Ma Weidong, Ye Qiwei, Liu Tie-Yan.* LightGBM: A Highly Efficient Gradient Boosting Decision Tree // Advances in Neural Information Processing Systems 30. 2017. 3146–3154.
- Lecun Y., Bottou L., Bengio Y., Haffner P.* Gradient-based learning applied to document recognition // Proceedings of the IEEE. 1998. 86, 11. 2278–2324.
- Lee Guang-He, Yuan Yang, Chang Shiyu, Jaakkola Tommi.* Tight Certificates of Adversarial Robustness for Randomly Smoothed Classifiers // Advances in Neural Information Processing Systems 32. 2019. 4910–4921.
- Madry Aleksander, Makelov Aleksandar, Schmidt Ludwig, Tsipras Dimitris, Vladu Adrian.* Towards Deep Learning Models Resistant to Adversarial Attacks // International Conference on Learning Representations. 2018.
- Prokhorenkova Liudmila, Gusev Gleb, Vorobev Aleksandr, Dorogush Anna Veronika, Gulin Andrey.* CatBoost: unbiased boosting with categorical features // Advances in neural information processing systems. 2018. 6638–6648.
- Smith J. Walter, Everhart James E., Dickson William C., Knowler William C, Johannes Richard S.* Using the ADAP Learning Algorithm to Forecast the Onset of Diabetes Mellitus // Proceedings of the Annual Symposium on Computer Application in Medical Care. 1988.
- Szegedy Christian, Zaremba Wojciech, Sutskever Ilya, Bruna Joan, Erhan Dumitru, Goodfellow Ian J., Fergus Rob.* Intriguing properties of neural networks // CoRR. 2013. abs/1312.6199.
- Tu Chun-Chen, Ting Pai-Shun, Chen Pin-Yu, Liu Sijia, Zhang Huan, Yi Jinfeng, Hsieh Cho-Jui, Cheng Shin-Ming.* AutoZOOM: Autoencoder-based Zeroth Order Optimization Method for Attacking Black-box Neural Networks // AACL. 2018.
- Wang De, Irani Danesh, Pu Calton.* Evolutionary study of web spam: Webb Spam Corpus 2011 versus Webb Spam Corpus 2006 // 8th International Conference on Collaborative Computing: Networking, Applications and Worksharing (CollaborateCom). 2012. 40–49.
- Wang Yihan, Zhang Huan, Chen Hongge, Boning Duane, Hsieh Cho-Jui.* On Lp-norm Robustness of Ensemble Decision Stumps and Trees // ICML. 2020.
- Xiao Han, Rasul Kashif, Vollgraf Roland.* Fashion-MNIST: a Novel Image Dataset for Benchmarking Machine Learning Algorithms. 2017.

Yang Yao-Yuan, Rashtchian Cyrus, Wang Yizhen, Chaudhuri Kamalika. Robustness for Non-Parametric Classification: A Generic Attack and Defense. 2019.

Zhang Fuyong, Wang Yi, Liu Shigang, Wang Hua. Decision-based evasion attacks on tree ensemble classifiers // World Wide Web. 04 2020.

Zhang Huan, Si Si, Hsieh Cho-Jui. GPU-acceleration for Large-scale Tree Boosting // arXiv preprint arXiv:1706.08359. 2017.

A Dataset and Model Statistics

We use 9 datasets and pre-trained models provided in Chen et al. (2019b), which can be downloaded from <https://github.com/chenhongge/RobustTrees>. Table 6 summarized the statistics of the datasets as well as the standard (natural) GBDT models, and we report the average complexity statistics for $|\text{Neighbor}_{\text{Bound}}(\cdot)|$ from 500 test examples. For multi-class datasets we count trees either belong to the victim class or the class of the initial adversarial example. Datasets may contain duplicate feature split thresholds and the extra complexity is covered in the statistics. We disabled the random noise optimization discussed in §3.5 to provide a cleaner picture of Algorithm 1. We train standard (natural) RF models using XGBoost’s native RF APIs¹, and provide the statistics in Table 7.

Table 6: The average complexity statistics for $|\text{Neighbor}_{\text{Bound}}(\cdot)|$ from 500 test examples.

| Dataset | features | classes | trees | depth l | iterations | $ T_{\text{Bound}}(\cdot) $ | $ \text{Neighbor}_1^{(t)}(\cdot) $ | $ \text{Neighbor}_{\text{Bound}}(\cdot) $ |
|---------------|----------|---------|-------|-----------|------------|-----------------------------|------------------------------------|---|
| breast-cancer | 10 | 2 | 4 | 6 | 2.1 | 3.2 | 5.2 | 9.2 |
| diabetes | 8 | 2 | 20 | 5 | 6.3 | 6.1 | 3.4 | 10.6 |
| MNIST2-6 | 784 | 2 | 1,000 | 4 | 121.7 | 374.2 | 14.9 | 256.5 |
| ijcnn | 22 | 2 | 60 | 8 | 26.5 | 7.4 | 3.3 | 17.8 |
| MNIST | 784 | 10 | 400 | 8 | 159.4 | 124.7 | 5.0 | 367.9 |
| F-MNIST | 784 | 10 | 400 | 8 | 236.8 | 149.1 | 6.5 | 717.4 |
| webspam | 254 | 2 | 100 | 8 | 100.7 | 37.0 | 3.8 | 129.7 |
| covtype | 54 | 7 | 160 | 8 | 36.7 | 30.8 | 10.6 | 39.2 |
| HIGGS | 28 | 2 | 300 | 8 | 107.1 | 13.5 | 2.1 | 24.0 |

Table 7: Parameters and statistics for datasets and the standard (natural) RFs.

| Dataset | train size | test size | trees | depth l | subsampling | test acc. |
|---------------|------------|-----------|-------|-----------|-------------|-----------|
| breast-cancer | 546 | 137 | 4 | 6 | .8 | .974 |
| diabetes | 614 | 154 | 25 | 8 | .8 | .775 |
| MNIST2-6 | 11,876 | 1,990 | 1000 | 4 | .8 | .963 |
| ijcnn | 49,990 | 91,701 | 100 | 8 | .8 | .919 |
| MNIST | 60,000 | 10,000 | 400 | 8 | .8 | .907 |
| F-MNIST | 60,000 | 10,000 | 400 | 8 | .8 | .823 |
| webspam | 300,000 | 50,000 | 100 | 8 | .8 | .948 |
| covtype | 400,000 | 180,000 | 160 | 8 | .8 | .745 |
| HIGGS | 10,500,000 | 500,000 | 300 | 8 | .8 | .702 |

B Supplementary Experiments

B.1 Additional Experimental Results on Random Forests

Table 8: Average ℓ_∞ perturbation over 100 test examples on the **standard (natural) random forests (RF) models**. Datasets are ordered by training data size. **Bold** and **blue** highlight the best and the second best entries respectively (not including MILP).

| Standard RF | Cube | | LT-Attack (Ours) | | MILP | | Ours vs. MILP | |
|---------------|-------------|--------------|------------------------|--------------|-------|-------|----------------------------|---------|
| | \bar{r} | time | \bar{r}_{our} | time | r^* | time | \bar{r}_{our}/r^* | Speedup |
| breast-cancer | .797 | .208s | .340 | .001s | .332 | .008s | 1.02 | 8X |
| diabetes | .159 | .271s | .111 | .002s | .103 | .054s | 1.08 | 27X |
| MNIST2-6 | .135 | 1.85s | .130 | .041s | .121 | .335s | 1.07 | 8.2X |
| ijcnn | .032 | .340s | .026 | .003s | .026 | .338s | 1.00 | 112.7X |
| MNIST | .017 | 1.98s | .010 | .056s | .009 | 21.4s | 1.11 | 382.1X |
| F-MNIST | .036 | 2.57s | .036 | .084s | .032 | 34.1s | 1.13 | 406X |
| webspam | .004 | .652s | .002 | .023s | .002 | 2.63s | 1.00 | 114.3X |
| covtype | .050 | .684s | .048 | .037s | .048 | 72.2s | 1.00 | 1951.4X |
| HIGGS | .008 | .389s | .007 | .011s | .006 | 20.9s | 1.17 | 1900X |

B.2 Attack Success Rate

We present attack success rate in Fig. 3, which is calculated as the ratio of constructed adversarial examples that have smaller perturbation than the thresholds. We use 50 test examples for MILP due to long running time, and 500 test examples for other methods.

¹https://xgboost.readthedocs.io/en/release_1.0.0/tutorials/rf.html

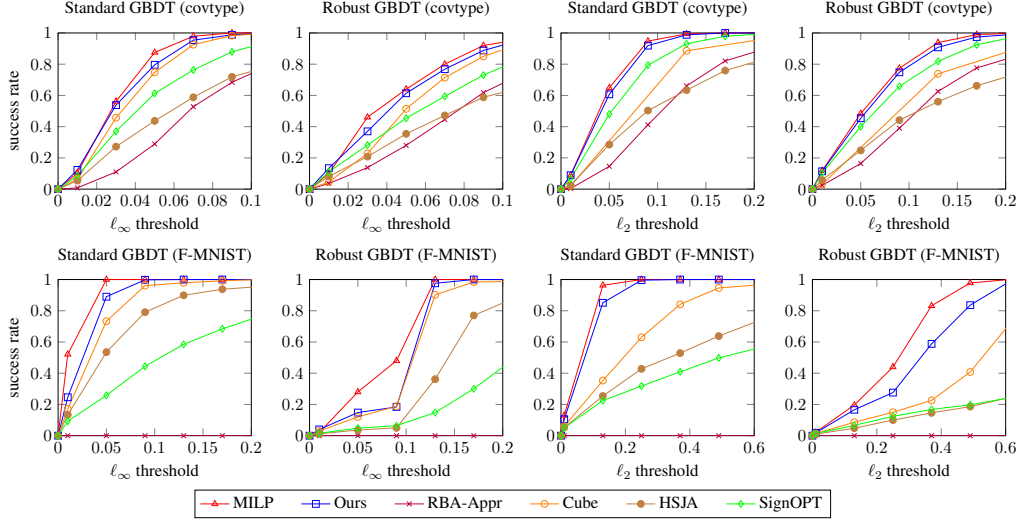


Figure 3: Attack success rate vs. perturbation thresholds.

B.3 ℓ_∞ Perturbation Using Different Number of Initial Examples

Fig. 4 presents the average ℓ_∞ perturbation of 50 test examples vs. runtime per test example in log scale. We plot the results for SignOPT, HSJA, Cube, and LT-Attack on $\{1, 2, 4, 6, 10, 20, 40\}$ initial examples, using 2 threads per task. Initial examples are not applicable to RBA-Appr and MILP thus we only plot a single point for each method.

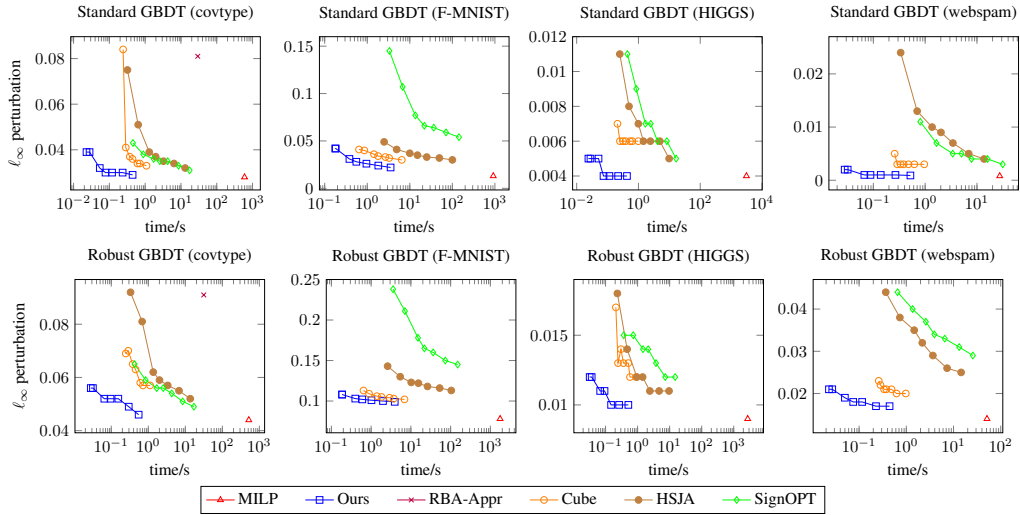


Figure 4: Average ℓ_∞ perturbation of 50 test examples vs. runtime per test example in log scale. Methods on the bottom-left corner are better.

B.4 Experimental Results for ℓ_1 Norm and Verification

Table 9 presents the experimental results on ℓ_1 norm perturbation. Cube doesn't support ℓ_1 objective by default and we report the ℓ_1 perturbation of the constructed adversarial examples from ℓ_∞ objective attacks. For completeness we include verification results (Chen et al., 2019b; Wang et al., 2020) in Table 9 and Table 10, which output lower bounds of the minimal adversarial perturbation denoted as \underline{r} (in contrast to adversarial attacks that aim to output an upper bound \bar{r}).

Table 9: Average ℓ_1 perturbation over 50 test examples on the **standard (natural) GBDT models** and **robustly trained GBDT models**. Datasets are ordered by training data size. **Bold** and **blue** highlight the best and the second best entries respectively (not including MILP and Verification).

| Standard GBDT | SignOPT | | RBA-Appr | | Cube | | LT-Attack (Ours) | | MILP | | Verification | | Ours vs. MILP | |
|---------------|-------------|-------|-----------|---------------|-------------|--------------|------------------------|--------------|-------|-------|-----------------|-------|----------------------------|----------|
| | \bar{r} | time | \bar{r} | time | \bar{r} | time | \bar{r}_{our} | time | r^* | time | \underline{r} | time | \bar{r}_{our}/r^* | Speedup |
| breast-cancer | .413 | .686s | .535 | .0002s | 1.02 | .234s | .372 | .002s | .372 | .012s | .367 | .003s | 1.00 | 6.X |
| diabetes | .183 | 1.04s | .294 | .0005s | .290 | .238s | .131 | .003s | .126 | .080s | .095 | .133s | 1.04 | 26.7X |
| MNIST2-6 | 35.4 | 6.81s | 25.9 | .109s | 3.73 | 3.47s | .783 | .230s | .568 | 2.51s | .057 | 1.17s | 1.38 | 10.9X |
| ijcnn | .075 | .889s | .286 | .016s | .247 | .340s | .064 | .008s | .060 | 3.28s | .044 | 1.68s | 1.07 | 410.X |
| MNIST | 22.8 | 8.77s | 46.5 | 3.13s | 2.16 | 7.11s | .341 | .267s | .207 | 56.8s | .013 | 5.40s | 1.65 | 212.7X |
| F-MNIST | 13.8 | 9.55s | 42.7 | 4.57s | 1.20 | 9.04s | .260 | .479s | .181 | 70.3s | .013 | 7.19s | 1.44 | 146.8X |
| webspam | .287 | 3.43s | .614 | .630s | .036 | 1.01s | .006 | .062s | .004 | 4.17s | .0003 | 6.40s | 1.50 | 67.3X |
| covtype | .074 | 1.74s | .223 | 2.29s | .132 | 1.01s | .057 | .039s | .052 | 314s | .024 | 2.26s | 1.10 | 8051.3X |
| HIGGS | .050 | 1.20s | .611 | 44.7s | .039 | .854s | .016 | .049s | .013 | 25min | .002 | 7.36s | 1.23 | 30183.7X |

| Robust GBDT | SignOPT | | RBA-Appr | | Cube | | LT-Attack (Ours) | | MILP | | Verification | | Ours vs. MILP | |
|---------------|-------------|-------|-------------|---------------|-------------|--------------|------------------------|--------------|-------|-------|-----------------|-------|----------------------------|----------|
| | \bar{r} | time | \bar{r} | time | \bar{r} | time | \bar{r}_{our} | time | r^* | time | \underline{r} | time | \bar{r}_{our}/r^* | Speedup |
| breast-cancer | .654 | .869s | .598 | .0008s | 1.23 | .210s | .574 | .002s | .574 | .008s | .506 | .001s | 1.00 | 4.X |
| diabetes | .201 | .667s | .228 | .001s | .514 | .235s | .189 | .002s | .189 | .028s | .166 | .007s | 1.00 | 14.X |
| MNIST2-6 | 23.8 | 6.51s | 17.8 | .106s | 6.69 | 3.47s | 2.76 | .523s | 1.78 | 23.2s | .381 | 2.91s | 1.55 | 44.4X |
| ijcnn | .076 | .693s | .205 | .015s | .233 | .337s | .067 | .007s | .065 | 1.02s | .043 | .279s | 1.03 | 145.7X |
| MNIST | 57.4 | 7.93s | 32.7 | 3.70s | 9.76 | 8.35s | 4.00 | .455s | 1.72 | 13min | .270 | 8.61s | 2.33 | 1652.7X |
| F-MNIST | 28.6 | 10.4s | 41.3 | 4.96s | 3.70 | 9.96s | 1.20 | .477s | .720 | 244s | .077 | 13.6s | 1.67 | 511.5X |
| webspam | .186 | 3.65s | .540 | .522s | .309 | 1.00s | .119 | .037s | .073 | 67.7s | .014 | 2.17s | 1.63 | 1829.7X |
| covtype | .097 | 1.65s | .217 | 2.43s | .241 | 1.02s | .080 | .075s | .071 | 437s | .033 | 3.12s | 1.13 | 5826.7X |
| HIGGS | .033 | 1.12s | .226 | 43.6s | .071 | .839s | .028 | .052s | .021 | 40min | .006 | 5.55s | 1.33 | 46576.9X |

Table 10: Average ℓ_∞ and ℓ_2 perturbation over 500 test examples on the standard (natural) GBDT models and robustly trained GBDT models. ("*"): Average of 50 examples due to long running time.

| Standard GBDT | LT-Attack (Ours) | | MILP | | Verification | | Robust GBDT | LT-Attack (Ours) | | MILP | | Verification | |
|---------------|------------------------|-------|-------|--------|-----------------|-------|---------------|------------------------|-------|-------|--------|-----------------|-------|
| | \bar{r}_{our} | time | r^* | time | \underline{r} | time | | \bar{r}_{our} | time | r^* | time | \underline{r} | time |
| breast-cancer | .235 | .001s | .222 | .013s | .220 | .002s | breast-cancer | .415 | .001s | .415 | .008s | .414 | .001s |
| diabetes | .059 | .002s | .056 | .084s | .047 | .910s | diabetes | .122 | .002s | .121 | .036s | .119 | .011s |
| MNIST2-6 | .097 | .222s | .065 | 28.7s | .053 | 1.27s | MNIST2-6 | .331 | .302s | .317 | 98.7s | .311 | 29.4s |
| ijcnn | .033 | .007s | .031 | 6.60s | .027 | 6.25s | ijcnn | .038 | .006s | .036 | 3.60s | .032 | .799s |
| MNIST | .029 | .237s | .014 | 375s* | .011 | 9.38s | MNIST | .298 | .315s | .278 | 13min* | .255 | 7.47s |
| F-MNIST | .028 | .370s | .013 | 15min* | .012 | 6.96s | F-MNIST | .098 | .403s | .078 | 29min* | .075 | 13.3s |
| webspam | .001 | .051s | .0008 | 27.5s | .0002 | 9.79s | webspam | .016 | .038s | .014 | 51.2s | .011 | 5.85s |
| covtype | .032 | .038s | .028 | 10min* | .021 | 4.21s | covtype | .047 | .053s | .044 | 518s* | .031 | 3.24s |
| HIGGS | .004 | .036s | .004 | 52min* | .002 | 13.2s | HIGGS | .01 | .054s | .009 | 45min* | .005 | 8.42s |

| Standard GBDT | LT-Attack (Ours) | | MILP | | Verification | | Robust GBDT | LT-Attack (Ours) | | MILP | | Verification | |
|---------------|------------------------|-------|-------|--------|-----------------|-------|---------------|------------------------|-------|-------|--------|-----------------|-------|
| | \bar{r}_{our} | time | r^* | time | \underline{r} | time | | \bar{r}_{our} | time | r^* | time | \underline{r} | time |
| breast-cancer | .283 | .001s | .280 | .011s | .277 | .002s | breast-cancer | .452 | .001s | .452 | .007s | .450 | .001s |
| diabetes | .077 | .003s | .073 | .055s | .058 | .458s | diabetes | .144 | .002s | .143 | .024s | .130 | .009s |
| MNIST2-6 | .245 | .235s | .183 | 2.52s | .058 | 1.06s | MNIST2-6 | .968 | .401s | .803 | 17.3s | .358 | 4.42s |
| ijcnn | .044 | .010s | .043 | 2.18s | .030 | 4.62s | ijcnn | .048 | .007s | .046 | .728s | .035 | .575s |
| MNIST | .072 | .243s | .043 | 32.5s | .013 | 6.81s | MNIST | .996 | .395s | .701 | 200s | .273 | 10.1s |
| F-MNIST | .073 | .400s | .049 | 49.3s | .013 | 6.72s | F-MNIST | .326 | .468s | .251 | 99.3s | .079 | 13.5s |
| webspam | .002 | .053s | .002 | 3.17s | .0002 | 8.95s | webspam | .039 | .036s | .033 | 12.0s | .012 | 4.72s |
| covtype | .045 | .039s | .042 | 237s | .023 | 2.96s | covtype | .063 | .054s | .059 | 280s | .033 | 3.10s |
| HIGGS | .008 | .037s | .007 | 13min* | .002 | 10.3s | HIGGS | .016 | .054s | .015 | 15min* | .006 | 7.16s |

C Proofs

C.1 Proof of Theorem 2

Proof. By contradiction. Given adversarial tuple \mathcal{C}' and victim example x_0 , assume

$$\exists \mathcal{C}_1 \in \text{Neighbor}_1^+(\mathcal{C}') \quad \text{s.t.} \quad \mathcal{C}_1 \notin \text{Neighbor}_{\text{Bound}}(\mathcal{C}').$$

Assume $p \in \{1, 2, \infty\}$. Let $x_1 = \text{argmin}_{x \in B(\mathcal{C}_1)} \|x - x_0\|_p$, $x' = \text{argmin}_{x \in B(\mathcal{C}')} \|x - x_0\|_p$, and let J be the set of dimensions that x_1 is closer to x_0 :

$$J = \{j \mid |x_{1,j} - x_{0,j}| < |x'_{j'} - x_{0,j}|\}.$$

According to the definition of $\text{Neighbor}_1^+(\mathcal{C}')$ we have $\text{dist}_p(\mathcal{C}_1, x_0) < \text{dist}_p(\mathcal{C}', x_0)$, and consequently $J \neq \emptyset$. We choose any $j' \in J$ and for cleanliness we use (l', r') to denote the interval from $B(\mathcal{C}')$ on j'_{th} dimension, and let $d_0 = x_{0,j'}$, $d_1 = x_{1,j'}$, $d' = x'_{j'}$.

Observe $d_0 \notin (l', r']$, otherwise we have $|d' - d_0| = 0$ and $|d_1 - d_0|$ cannot be smaller. W.l.o.g. assume d_0 is on the right side of the interval, i.e., $r' < d_0$, then according to the argmin property of x' we have $d' = r'$.

Recall that $B(\mathcal{C}')$ is the intersection of K bounding boxes from the ensemble, then

$$\exists t' \in [K] \quad \text{s.t.} \quad B_{j'}^{\mathcal{C}'(t')} \cdot r = r'.$$

Observe $r' = d' < d_1$ since d_0 is on the right side of d' and d_1 has smaller distance to d_0 , which means \mathcal{C}_1 has different leaf than \mathcal{C}' on tree t . Also according to the above equation $t' \in T_{\text{Bound}}(\mathcal{C}')$, and $\mathcal{C}_1 \in \text{Neighbor}_1^{(t')}(\mathcal{C}')$, thus $\mathcal{C}_1 \in \bigcup_{t \in T_{\text{Bound}}(\mathcal{C}')} \text{Neighbor}_1^{(t)}(\mathcal{C}') = \text{Neighbor}_{\text{Bound}}(\mathcal{C}')$, contradiction. \square

C.2 Proof of Corollary 2

Proof. According to Theorem 1 $B^{(-t)}$ is the intersection of $K - 1$ bounding boxes and can be written as the Cartesian product of d intervals, we call it a *box*. Each tree t of depth l splits the \mathbb{R}^d space into up to 2^l non-overlapping axis-aligned boxes, and $|\text{Neighbor}_1^{(t)}(\mathcal{C}')| + 1$ (plus current box) corresponds to the number of boxes that has non-empty intersection with $B^{(-t)}$, thus $|\text{Neighbor}_1^{(t)}(\mathcal{C}')| \leq 2^l - 1$.

Observe that $k^{(t)}$ axis-aligned feature split thresholds can split \mathbb{R}^d into at most $2^{k^{(t)}}$ non-overlapping boxes, assuming $d \geq k^{(t)}$, and the maximum can be reached by having at most 1 split threshold on each dimension. In conclusion there are at most $2^{\min(k^{(t)}, l)}$ boxes that has non-empty intersection with $B^{(-t)}$, thus $|\text{Neighbor}_1^{(t)}(\mathcal{C}')| \leq 2^{\min(k^{(t)}, l)} - 1$ (minus the current box). \square

C.3 Proof of Theorem 3

Proof. By contradiction. Let x_0, y_0 be the victim example and assume

$$\exists \mathcal{C}^* \in (V^+)^K \cap \mathbb{C} \quad \text{s.t.} \quad f(\mathcal{C}^*) \neq y_0 \wedge \text{dist}_p(\mathcal{C}^*, x_0) < \text{dist}_p(\mathcal{C}', x_0).$$

Assume $p \in \{1, 2, \infty\}$. Recall $f(\mathcal{C}) = \text{sign}(\sum_{i \in \mathcal{C}} v^i)$, we compute the tree-wise prediction difference

$$v_{\text{diff}}^{(t)} = v^{\mathcal{C}^{*(t)}} - v^{\mathcal{C}'(t)}, \quad t \in [K].$$

Let t_{\min} be the tree with the smallest functional margin difference

$$t_{\min} = \underset{t \in [K]}{\text{argmin}} \quad y_0 \cdot v_{\text{diff}}^{(t)}.$$

We construct a tuple \mathcal{C}_1 which is the same as \mathcal{C}' except on t_{\min} , where $\mathcal{C}_1^{(t_{\min})} = \mathcal{C}^{*(t_{\min})}$, consequently we have

$$\mathcal{C}_1 \in \mathbb{C} \wedge \text{dist}_p(\mathcal{C}_1, x_0) < \text{dist}_p(\mathcal{C}', x_0).$$

Now we show $f(\mathcal{C}_1) \neq y_0$, or $y_0 \sum_{i \in \mathcal{C}_1} v^i < 0$:

i. Case $y_0 \cdot v_{\text{diff}}^{(t_{\min})} \leq 0$. Then

$$y_0 \sum_{i \in \mathcal{C}_1} v^i = y_0 \sum_{i \in \mathcal{C}'} v^i + y_0 \cdot v_{\text{diff}}^{(t_{\min})} \leq y_0 \sum_{i \in \mathcal{C}'} v^i < 0.$$

ii. Case $y_0 \cdot v_{\text{diff}}^{(t_{\min})} > 0$. Then

$$\begin{aligned} y_0 \sum_{i \in \mathcal{C}_1} v^i &= y_0 \sum_{i \in \mathcal{C}'} v^i + y_0 \cdot v_{\text{diff}}^{(t_{\min})} < y_0 \sum_{i \in \mathcal{C}'} v^i + K y_0 \cdot v_{\text{diff}}^{(t_{\min})} \\ &\leq y_0 \sum_{i \in \mathcal{C}'} v^i + y_0 \sum_{t \in [K]} v_{\text{diff}}^{(t)} = y_0 \sum_{i \in \mathcal{C}^*} v^i < 0. \end{aligned}$$

In conclusion \mathcal{C}_1 is a valid adversarial tuple within $\text{Neighbor}_1(\mathcal{C}')$ and has smaller perturbation than \mathcal{C}' , thus the algorithm won't stop. \square

D Supplementary Algorithms

D.1 Generating Initial Adversarial Examples for LT-Attack

Algorithm 2: Generating Initial Adversarial Examples for LT-Attack

Data: Target white-box model f , victim example x_0 .

```

1 begin
2    $y_0 \leftarrow f(x_0)$ ;
3    $r', C' \leftarrow MAX, None$ ;
4    $num\_attack \leftarrow 20$ ;
5   for  $i \leftarrow 1, \dots, num\_attack$  do
6     do
7        $x' \leftarrow x_0 + Normal(0, 1)^d$ ;
8       while  $f(x') = y_0$ ;
9        $x' \leftarrow BinarySearch(x', x_0, f)$ ;
10       $\triangleright$  Do a fine-grained binary search between  $x_0$  and  $x'$  to optimize the initial perturbation of  $x'$ .
11      Similar to  $g(\theta)$  proposed by Cheng et al. (2019).
12       $r^*, C^* \leftarrow LT-Attack(f, x_0, x')$ ;
13      if  $r^* < r'$  then
14         $r', C' \leftarrow r^*, C^*$ ;
15      end
16    end
17  end
18  return  $r', C'$ 
19 end

```

D.2 Algorithm for NaiveLeaf

Algorithm 3: Compute NaiveLeaf

Data: Target white-box model f , current adversarial example x' , victim example x_0 .

Result: The NaiveLeaf neighborhood of $\mathcal{C}(x')$

```

1 begin
2    $(i^{(1)}, \dots, i^{(K)}) \leftarrow \mathcal{C}(x')$ ;
3    $N \leftarrow \emptyset$ ;
4   for  $t \leftarrow 1 \dots K$  do
5     for  $i \in S^{(t)}, i \neq i^{(t)}$  do
6        $\triangleright S^{(t)}$  denotes the leaves of tree  $t$ .
7        $x_{new} \leftarrow x'$ ;
8       for  $j, (l, r) \in B^i$  do
9          $\triangleright$  The  $j$ th dimension of the bounding box  $B^i$ , can be acquired from  $f$ .
10        if  $x_{new,j} \notin (l, r]$  then
11           $x_{new,j} \leftarrow \min(r, \max(l + \epsilon, x_{0,j}))$ ;
12        end
13      end
14       $N \leftarrow N \cup \{C(x_{new})\}$ ;
15    end
16  end
17  return  $N$ 
18 end

```

D.3 A Greedy Algorithm to Estimate the Minimum Neighborhood Distance

To understand the quality of constructed adversarial examples we use an empirical greedy algorithm to estimate the minimum *neighborhood distance* h such that $\text{Neighbor}_h(\cdot)$ can reach the *exact* solution. Assume our method converged at \mathcal{C}' and the optimum solution is \mathcal{C}^* , let $T_{\text{diff}} = \{t \mid \mathcal{C}'^{(t)} \neq \mathcal{C}^{*(t)}\}$ be the set of trees with different prediction, then the Hamming distance $\bar{h} = |T_{\text{diff}}|$ is a trivial upper bound where $\text{Neighbor}_{\bar{h}}(\mathcal{C}')$ can reach \mathcal{C}^* with a single addition iteration. To estimate a realistic $h \sim \bar{h}$ we want to find the disjoint split $T_{\text{diff}} = \cup_{i \in [k]} T_i$ such that we can mutate \mathcal{C}' into \mathcal{C}^* by changing trees in T_i to match \mathcal{C}^* at i_{th} iteration. We make sure all intermediate tuples are valid and has strictly

decreasing perturbation as required by Eq. (3), and report $h^\sim = \max_{i \in [k]} |T_i|$. h^\sim is an estimation of the minimum h because we cannot guarantee the argmin constrain due to the large complexity. As shown in Table 11 we have $median(\bar{h}) = 23$ and $median(h^\sim) = 8$ on ensemble with 300 trees (HIGGS), which suggests that our method is *likely* to reach the exact optimum on half of the test examples through ~ 3 additional iterations on $Neighbor_8(\cdot)$. In this experiment we disabled the random noise optimization discussed in §3.5 to provide a cleaner picture of Algorithm 1.

Algorithm 4: A greedy algorithm to estimate the minimum neighborhood distance h^\sim .

Data: The model f , our adversarial point x_{our} , exact MILP solution x^* .

Result: An estimation of neighborhood distance h^\sim .

```

1 begin
2    $C_{our}, C^* \leftarrow \mathcal{C}(x_{our}), \mathcal{C}(x^*);$ 
3    $r^* \leftarrow \text{dist}_p(C^*, x_0);$ 
4    $y^* \leftarrow f(x^*);$ 
5    $h_{min} \leftarrow D(C_{our}, C^*);$  ▷ Hamming distance is the upper bound.
6    $I_{diff} \leftarrow \{(v^{C^{*(t)}} - v^{C_{our}^{(t)}}, C_{our}^{(t)}, C^{*(t)}) \mid C_{our}^{(t)} \neq C^{*(t)}, t \in [K]\};$ 
▷  $I_{diff}$  is the list of tuples in the form of (label diff, our leaf, MILP leaf).
7    $num\_trial \leftarrow 200;$ 
8   for  $i \leftarrow 1, \dots, num\_trial$  do
9      $h \leftarrow 0;$ 
10     $I \leftarrow \text{shuffle}(I_{diff});$ 
11     $C_{tmp} \leftarrow C_{our};$ 
12    while  $I \neq \emptyset$  do
13       $r_{last} \leftarrow \text{dist}_p(C_{tmp}, x_0);$ 
14       $C_{tmp} \leftarrow \text{pop the first tuple from } I \text{ with positive label diff and replace with MILP leaf};$ 
15       $h \leftarrow h + 1;$ 
16      while  $C_{tmp} \notin \mathcal{C}$  or  $\text{dist}_p(C_{tmp}, x_0)_p \notin [r^*, r_{last}]$  or  $f(C_{tmp}) \neq y^*$  do
▷ Making sure  $C_{tmp}$  satisfies Equation 3 except the argmin. We cannot guarantee
argmin due to the high complexity. The while loop is guaranteed to exit since we
can pop all tuples in  $I$  to become  $C^*$ .
17       $C_{tmp} \leftarrow \text{pop the first tuple from } I \text{ and replace with MILP leaf};$ 
18       $h \leftarrow h + 1;$ 
19    end
20  end
21   $h_{min} \leftarrow \min(h_{min}, h);$ 
22 end
23 return  $h_{min}$ 
24 end

```

Table 11: Convergence statistics for the standard (natural) GBDT models between our solution and the optimum MILP solution. We collect the data after the fine-grained binary search but before applying LT-Attack (Initial), and the data after LT-Attack (Converged). We disabled the random noise optimization discussed in §3.5.

| Dataset | Model | HammingDist \bar{h} | | | | NeighborDist h^\sim | | | |
|---------------|-------|-----------------------|-----|-----------|-----|-----------------------|-----|-----------|-----|
| | | Initial | | Converged | | Initial | | Converged | |
| | | # of trees | max | median | max | median | max | median | max |
| breast-cancer | 4 | 2 | 0 | 0 | 0 | 2 | 0 | 0 | 0 |
| diabetes | 20 | 10 | 3 | 6 | 0 | 5 | 1 | 4 | 0 |
| MNIST2-6 | 1000 | 676 | 490 | 347 | 172 | 172 | 46 | 64 | 36 |
| ijcnn | 60 | 27 | 10 | 16 | 3 | 18 | 2 | 8 | 2 |
| MNIST | 400 | 266 | 115 | 96 | 33 | 173 | 8 | 12 | 7 |
| F-MNIST | 400 | 237 | 174 | 100 | 56 | 82 | 12 | 18 | 10 |
| webspam | 100 | 88 | 56 | 36 | 16 | 75 | 7 | 9 | 4 |
| covtype | 160 | 84 | 23 | 67 | 9 | 82 | 7 | 65 | 6 |
| HIGGS | 300 | 190 | 62 | 125 | 23 | 181 | 12 | 121 | 8 |